

Article

Eddy Current Mechanism Model for Dynamic Magnetic Field in Ferromagnetic Metal Structures

Chao Zuo ^{1,2}, Zhipeng Lai ³, Zuoshuai Wang ^{1,2}, Jianxun Wang ^{1,2}, Hanchen Xiao ^{1,2}, Wentie Yang ^{1,2}, Pan Geng ^{1,2} and Meng Chen ^{1,2,*}

¹ Wuhan Second Ship Design & Research Institute, Wuhan 430205, China; csszc@foxmail.com (C.Z.); hustwzs@foxmail.com (Z.W.); wangcoven7@163.com (J.W.); onlyxhc1217@163.com (H.X.); yangwentie2024@163.com (W.Y.); perfectpg2024@outlook.com (P.G.)

² Hubei Key Laboratory of Marine Electromagnetic Detection and Control, Wuhan 430205, China

³ Wuhan National High Magnetic Field Center, Huazhong University of Science & Technology, Wuhan 430074, China; zplai@hust.edu.cn

* Correspondence: chenmeng2you@outlook.com

Abstract: The degaussing process is crucial for ensuring magnetic protection in ships. It involves the application of oscillating and attenuating magnetic fields to eliminate residual magnetism in the ship's structure. However, this process can lead to the generation of distorted magnetic fields within the ship's cabin, posing a potential threat to electronic equipment performance. Therefore, it is essential to have a comprehensive understanding of the dynamic magnetic field response in ship structures to develop effective degaussing systems. To address this need, this paper proposes an eddy current model for analyzing the dynamic magnetic field response in ferromagnetic metal structures. This model focuses on the role of eddy currents in shaping the magnetic field response and provides valuable insights into the underlying mechanisms. Using the proposed eddy current model, the effects of key system parameters such as thickness, conductivity, and the length-scale of the ship structure can be analytically investigated. This analysis helps in understanding how these parameters influence the dynamic magnetic field response and aids in the design and optimization of degaussing systems. The effectiveness and applicability of the proposed eddy current model are demonstrated through comprehensive investigations involving two simulation cases of varying complexity. The model accurately predicts the changing trends of the dynamic magnetic field response, as confirmed through finite element simulations. This validation highlights the model's ability to reproduce simulation results accurately and its potential as a powerful tool for analyzing and optimizing dynamic magnetic field responses. In summary, the proposed eddy current model represents a significant advancement in the field. It provides a valuable theoretical framework for understanding and analyzing the dynamic magnetic field response in ferromagnetic metal structures. By offering insights into the underlying mechanisms and the influence of key parameters, this research contributes to the development of improved degaussing systems and enhances the overall magnetic protection capabilities of ships.

Keywords: magnetic field; eddy current; ferromagnetic; magnetization; equivalent circuit; dynamic magnetic response



Citation: Zuo, C.; Lai, Z.; Wang, Z.; Wang, J.; Xiao, H.; Yang, W.; Geng, P.; Chen, M. Eddy Current Mechanism Model for Dynamic Magnetic Field in Ferromagnetic Metal Structures.

Electronics **2024**, *13*, 3772. <https://doi.org/10.3390/electronics13183772>

Academic Editor: Farhad Rachidi

Received: 22 January 2024

Revised: 6 May 2024

Accepted: 16 May 2024

Published: 23 September 2024



Copyright: © 2024 by the authors. Licensee MDPI, Basel, Switzerland. This article is an open access article distributed under the terms and conditions of the Creative Commons Attribution (CC BY) license (<https://creativecommons.org/licenses/by/4.0/>).

1. Introduction

Ships are predominantly constructed using ferromagnetic metal structures, which inherently retain residual magnetism. This residue magnetism can be problematic and even perilous in certain situations, particularly within the military domain. In military applications, the residue magnetism of a ship can be exploited by adversaries for the purpose of detecting the vessel using magnetic probes [1–4]. Consequently, degaussing has become a fundamental requirement for protecting ships against magnetic detection in military operations, which involves employing an oscillating and attenuating magnetic

field with amplitudes 15–50 times stronger than the Earth’s geomagnetic field to eliminate the residual magnetism from the ship’s structure, as shown in Figure 1 [5–7].

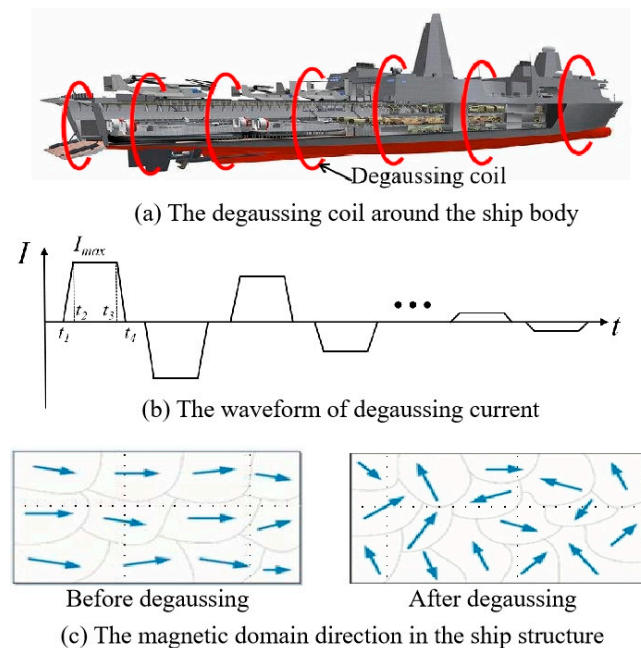


Figure 1. Schematic diagram of ship degaussing process.

However, the degaussing process also induces a complex electromagnetic field within the internal compartments of the ship, posing a potential threat to the functionality and performance of electronic equipment housed within [8]. Therefore, it is crucial to develop a thorough understanding of the dynamic magnetic field response of the ship’s structure to advance high-performance degaussing systems.

Finite element calculations have been employed to study the magnetic field response in ships [9–11]. However, due to the intricate nature of ship structures, these calculations are accompanied by high modeling costs and computational challenges. Current approaches simplify the models by neglecting structural details and employing shell elements, but these simplifications lack theoretical guidance. Furthermore, even with these simplifications, conventional finite element calculations for ship structures still involve millions of degrees of freedom, requiring approximately 50 h for static analysis and incurring substantial computational costs. Moreover, the practical degaussing process may last up to 100 s and involve rapid changes similar to step excitation which involves a wide frequency spectrum. Consequently, the cost of conducting comprehensive dynamic simulation calculations is prohibitively high, limiting research on the dynamic magnetic field response of ships. Currently, there are no systematic reports or comprehensive understanding of this field.

To address this issue, the main objective of this paper is to propose an analytical model for comprehending the dynamic magnetic field response of ships. This model aims to quantitatively evaluate the time constant of magnetic field dynamics, guide appropriate model simplifications, and determine optimal computational parameter settings. Based on fundamental electromagnetic principles, one of the most fundamental phenomena in the dynamic magnetic field response of ferromagnetic metal structures is the eddy current effect. Eddy currents induce a complex magnetic field in the surrounding space and can be a key mechanism for observed distortions in the magnetic field inside the ship’s ferromagnetic structures. In other areas, such as electromagnetic forming, there have been quantitative investigations on the effects of eddy currents. In these investigations, the ratio between the conductor’s thickness and skin depth has been widely used to assess the magnetic field shielding effect of eddy currents [12]. However, this ratio only considers a few parameters and neglects the overall geometry and scale length of the structure, thereby

inadequately capturing the dynamic magnetic field response resulting from changes in dimensional parameters. To overcome this limitation, a universal equivalent circuit model was proposed by Lai et al. [13], in which the magnetic field shielding effect was reflected by the ratio of inductance impedance to resistance. This model incorporates the magnetic flux coupling effect and dimensional parameters of the conductor material in the calculation of inductance and resistance [14–17], making it more versatile and practical.

This paper focuses on the investigation of the dynamic magnetic field response of ferromagnetic structures through numerical and analytical analysis based on the equivalent circuit model initially developed by Lai et al. [13]. The study explores the effects of system parameters, including conductivity, permeability, and dimensional parameters, on the dynamic magnetic field response of the ferromagnetic structure [18–20]. Furthermore, a detailed analysis of the variation of magnetic field and eddy current with different scaling ratios of dimensional parameters is conducted to unveil general scaling criteria for the dynamic magnetic field response of ferromagnetic structures. The findings of this study provide guidance for model simplification, scaled model manufacturing, and the rapid assessment of dynamic magnetic field response.

2. Proposed Eddy Current Mechanism Model

The main hypothesis of this paper is that the eddy current effect plays a dominant role in shaping the dynamic magnetic field within the ferromagnetic metal structures of a ship. A commonly used model for understanding the eddy current phenomenon is the skin depth effect, which explains how the dynamic magnetic field penetrates the metal conductors at different excitation frequencies. The skin depth is quantitatively calculated using the following formula:

$$\delta_s = \frac{1}{\sqrt{\pi f \sigma \mu}} \quad (1)$$

where f is the excitation frequency, σ is the material conductivity, and μ is the material permeability.

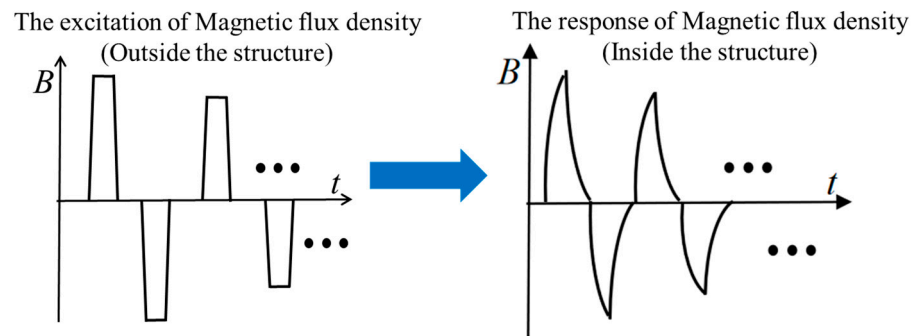
While Equation (1) quantifies the effects of material properties and excitation frequency, it does not consider the impact of the overall geometry and scale of the structures. Consequently, it fails to fully capture the dynamics involved.

To address this limitation, another eddy current mechanism, known as the equivalent RL circuit model, is proposed in this study [14–17]. This mechanism assumes that the dynamic magnetic field effects on the ferromagnetic structure are primarily caused by dynamic excitations, such as step excitations, as shown in Figure 2a. The model consists of a voltage source (U) representing the impact electromotive force, a resistance (R) representing the Ohmic loss due to eddy currents, and an inductance (L) representing the effect of eddy current-induced magnetic fields. When a step magnetic field is applied, the voltage source (U) generates a Dirac function signal (with an infinitely large value and infinitesimally small pulse width but finite energy) in the circuit, resulting in the immediate induction of a finite eddy current. Subsequently, the eddy current follows the evolution law of a first-order RL dynamic circuit, decaying exponentially, as shown in Figure 2b. The decay coefficient represents the time constant of the LR circuit and is expressed as follows:

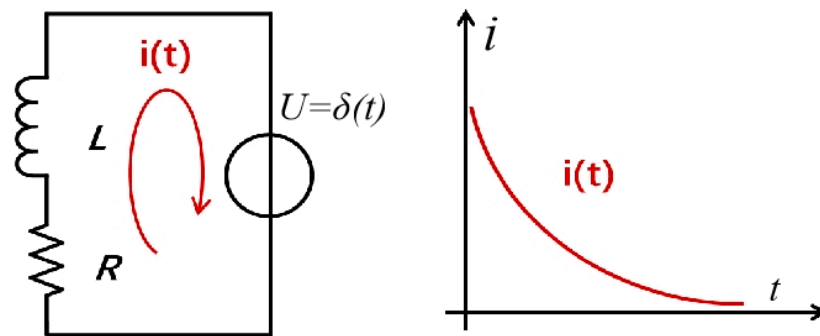
$$T = \frac{L}{R} \quad (2)$$

This model considers the equivalent inductance (L) and resistance (R) as functions of system parameters, directly reflecting the influence of geometric and material properties on the dynamic magnetic field characteristics. Consequently, the derived time constant can effectively capture the impact of system parameters on the dynamic magnetic field response time constant. In the following sections, we derive the analytical expressions for the equivalent inductance and resistance using a simple hollow cylinder structure as an example. It is important to note that this mechanism model is not limited to simple structures but is proposed to guide the modeling of more complex structures. The choice

of a simple structure here is to provide explicit analytical expressions explicitly related to structural parameters and validate the effectiveness of the mechanism model through finite element calculations on the simplified model. Once validated, this mechanism model can be used to guide the simplification of complex structure models by focusing on the structures related to the system’s R and L parameters while simplifying features unrelated to the relationship.



(a) The distortions of the magnetic flux density waveform



(b) The L-R equivalent circuit model and its eddy current waveform

Figure 2. Schematic diagram of the eddy current mechanism model.

Figure 3 presents the dimensional parameters of the hollow cylinder considered in deriving the analytical expression for the eddy current mechanism model. The cylinder has a height (a), an outer radius (b), and a thickness (c), where c is significantly smaller than b . The eddy current flows in the circumferential direction along the cylinder surface, leading to a magnetic field distribution similar to that of a solenoid coil. Although the material is ferromagnetic, for simplicity, we neglect the influence of its magnetic permeability on the spatial magnetic field. This assumption is reasonable since $c \ll b$, meaning that the ferromagnetic material occupies a small proportion of the entire space. In fact, the cylinder model in Figure 3 is to simulate the ship structure in which we neglected lots of structure details. And in actual ship structure, the overall size of the structure would be greater than the thickness of the structure by more than two orders. Therefore, this assumption holds true for actual ships as well.

Based on these settings, we can derive the analytical expressions for the equivalent inductance and resistance as follows [14]:

$$R = k_1 \frac{2\pi b}{\sigma ac} \tag{3}$$

$$L = k_2 \frac{\mu_0 \pi b^2}{a} \tag{4}$$

where σ is the conductivity of the hollow cylinder and k_1 and k_2 are the modified coefficients. k_1 reflects the effects of the skin depth and the flow path of the eddy current. k_2 reflects the effects of the finite height of the cylinder on the magnetic flux leakage.

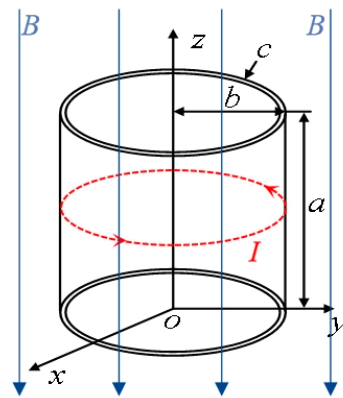


Figure 3. Dimensional parameters of the hollow cylinder.

In fact, k_1 and k_2 would not be constant but should be the function of the geometry parameter of the system. However, this would result in a very complicated expression for Equations (3) and (4), making it difficult to show the influencing laws of geometry parameters on the equivalent resistance (R) and inductance (L) and the resultant time constant. On the other hand, when maintaining the geometry parameter with a specific scope, their effects on k_1 and k_2 can be limited; in this way, neglecting these effects would not substantially change R , L , and t .

By substituting Equations (3) and (4) into Equation (2), we obtain the analytical expression for the time constant of the eddy current effect as follows:

$$T = \frac{L}{R} = \frac{\mu_0 k_2}{2k_1} \sigma b c \quad (5)$$

Based on Equation (5), the following deductions can be drawn regarding the eddy current mechanism model:

The time constant (T) is positively proportional to the material conductivity. Higher conductivity results in smaller resistance, leading to more significant eddy currents induced by dynamic magnetic field excitations and a more pronounced lag effect in the dynamic magnetic field.

The time constant (T) is positively proportional to the outer radius (b). According to Equations (3) and (4), resistance (R) is proportional to the outer radius (b), while inductance (L) is proportional to the square of the outer radius (b). Therefore, the outer radius (b) has a greater impact on inductance (L) than on resistance (R). As the outer radius (b) increases, inductance (L) significantly increases, resulting in a higher time constant (T) and a more pronounced lag effect in the dynamic magnetic field.

The time constant (T) is positively proportional to the thickness (c). The change in thickness (c) primarily affects resistance (R) and has a minimal impact on inductance (L). Consequently, when scaling the geometry with equal thickness for ferromagnetic materials, the variation in the time constant (T) becomes more significant, leading to a more pronounced lag effect in the dynamic magnetic field.

Right now, we have analytically derived and analyzed the proposed eddy current mechanism model using a hollow cylindrical ferromagnetic structure. In the subsequent sections, we will validate its effectiveness by comparing it with the results obtained through finite element simulations.

3. Validation on the Eddy Current Mechanism Model I: Single-Layer Ferromagnetic Structure

To validate the proposed eddy current mechanism model, two ferromagnetic structures have been designed, and the time constant of the dynamic magnetic field is used as an evaluation index for quantifying the model's effectiveness.

For simplicity, the adopted structures have an axisymmetric design, which helps reduce the computational cost of finite element analysis. As mentioned earlier, actual military ship structures are too complex to be simulated within a reasonable time. Additionally, using simplified structures is necessary to comply with military confidentiality requirements, as the detailed structures of military ships cannot be publicly shared.

To manage the complexity of the structures, we vary the number of layers. In this section, we analyze a single-layer structure, while the multiple-layer structure will be analyzed in the next section.

3.1. Basic Examples

Figure 4 and Table 1 present the system parameter setup for the adopted single-layer ferromagnetic structure. The simulation process is conducted using COMSOL Multiphysics, with a Helmholtz coil applying the excitation magnetic field to the structure.

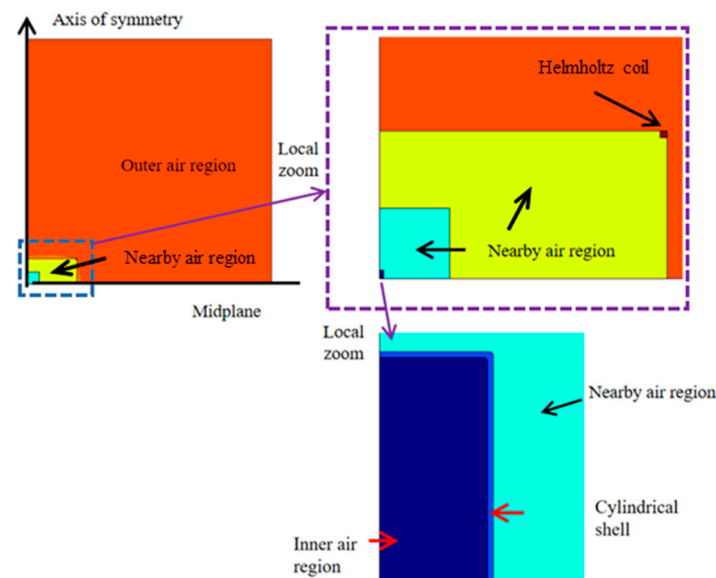


Figure 4. 2-dimensional axisymmetric model of the simple ferromagnetic structure.

Table 1. The dimensions and electromagnetic parameters of the cylinder.

Radius	Height	Thickness	Conductivity	Relative Permeability
0.3 m	1.2 m	30 mm	5.9×10^6 S/m	80

As shown in Figure 5, a step-function excitation is applied to the Helmholtz coil, generating a step-function magnetic flux density (with a magnitude of 35×10^{-4} T) in the structures. Figure 5b illustrates the magnetic field response at the center of the cylinder, while Figure 5c depicts the eddy current response in the ferromagnetic structure. It is evident that both the magnetic field and the eddy current exhibit significant delay characteristics in response to the step-function excitation. Notably, the magnetic field response exhibits a time constant similar to that of the eddy current response, approximately 0.35 s. This suggests a strong correlation between the magnetic dynamics and the evolution of the eddy current, which aligns with the proposed eddy current mechanism model. The model suggests that the induced eddy current is responsible for the dynamics of the magnetic

field inside the ship. In the subsequent subsections, we will quantitatively validate the effectiveness of the proposed eddy current model through parametric analysis.

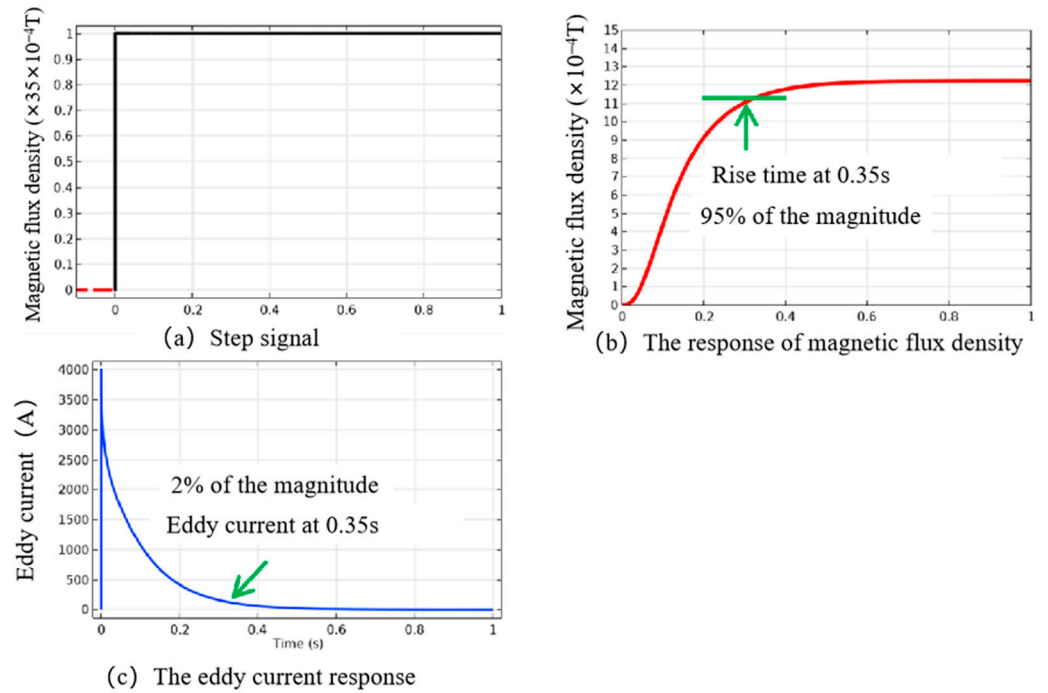


Figure 5. Typical response curve under the excitation of step signal.

3.2. Effects of Conductivity on the Dynamic Magnetic Field Response

Parametric analysis begins by varying the conductivity of the structure. As shown in Table 2, six typical conductivities of the model were selected, ranging from 1/20 to two times the base-line conductivity value (5.9×10^6 S/m). Figure 6 shows the dynamic responses of the magnetic flux density and the eddy current under different conductivity, while Figure 7 explicitly illustrates the variations in amplitude and time constant of the magnetic field and the eddy current waveform with respect to conductivity.

Table 2. The dimensions and electromagnetic parameters of the model.

Radius	Height	Thickness	Conductivity	Relative Permeability
0.3 m	1.2 m	30 mm	Reference: 5.9×10^6 S/m Relative value: 1/20, 1/10, 1/5, 1/2, 1, 2	80

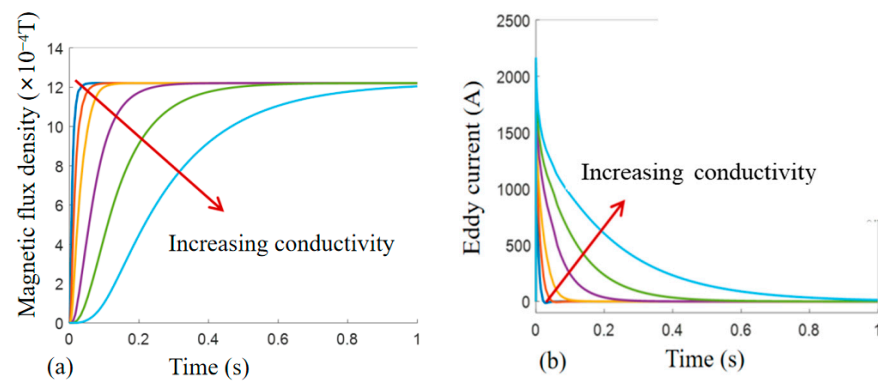


Figure 6. The change of magnetic flux density (a) and eddy current (b) with time at different conductivity.

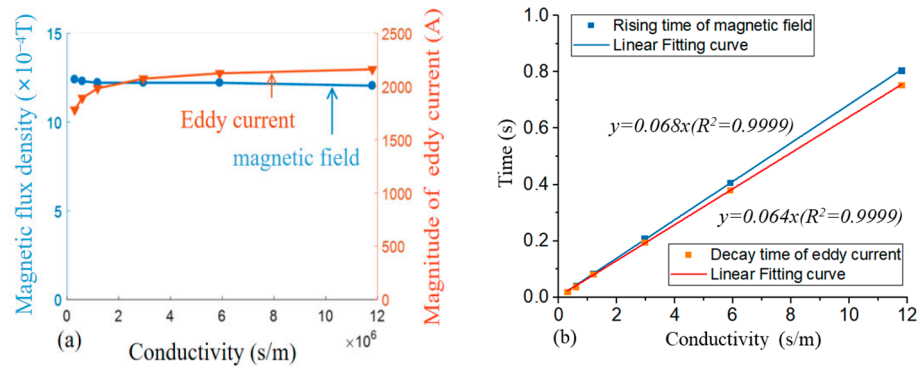


Figure 7. The magnitude (a) and characteristic time (b) of magnetic flux density and eddy current at different conductivity.

As shown in Figure 7a, it is worth noting that conductivity has little influence on the amplitude of the magnetic field and the eddy current. In fact, the peak of the eddy current is observed at the beginning of the waveform, after which it rapidly decayed, as shown in Figure 6b. This eddy current is excited by the step-function signal of the external magnetic field, which is dominated by a high frequency component. Additionally, for the equivalent RL circuit that is excited by the high frequency signal, the equivalent impedance of the inductance L ($2\pi fL$) would be much greater than the impedance of the resistance R . In this way, the amplitude of the eddy current is dominated by the impedance of the L but not R , making it only weak relative to the conductivity. The amplitude of the magnetic field inside the cylinder is correlated to the amplitude of the eddy current, so it is also only weakly affected by the conductivity.

However, the conductivity significantly affects the rise time of the magnetic field (reaching 95% of its magnitude) and the decay time of the eddy current (reaching 2% of its magnitude) (Figure 7b). Moreover, the time constant for both the magnetic field and the eddy current shows a clear linear relationship with conductivity, and they agree very well with each other. This observation confirms the deduction made in Equation (5) regarding the proportional relationship between the time constant and conductivity.

3.3. Effects of Thickness on the Dynamic Magnetic Field Response

The parametric analysis continues by varying the thickness of the structure. As shown in Table 3, six values of structure thickness have been scheduled in simulations, ranging from 1–50 mm. Figure 8 shows the dynamic responses of the magnetic flux density and the eddy current under different thicknesses, while Figure 9 explicitly demonstrates the variations in amplitude and time constant of the magnetic field and the eddy current with respect to thickness.

Table 3. The dimensions and electromagnetic parameters of the model.

Radius	Height	Thickness	Conductivity	Relative Permeability
0.3 m	1.2 m	Reference: 30 mm	5.9×10^6 S/m	80
		Absolute value: 1, 2, 5, 10, 30, 50 mm		

It is worth noting that the thickness of the structure significantly affects the rise time of the magnetic field and the decay time of the eddy current (as shown in Figure 9b). Moreover, the time constant for both the magnetic field and the eddy current exhibits a clear linear relationship with the thickness and shows excellent agreement. This observation further confirms the deduction made in Equation (5) regarding the proportional relationship between the time constant and the thickness.

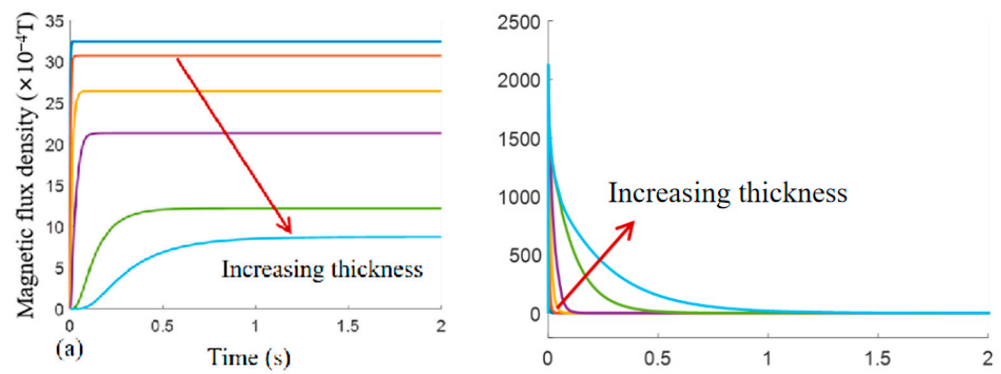


Figure 8. The changes in magnetic flux density (a) and eddy current (b) at different thicknesses.

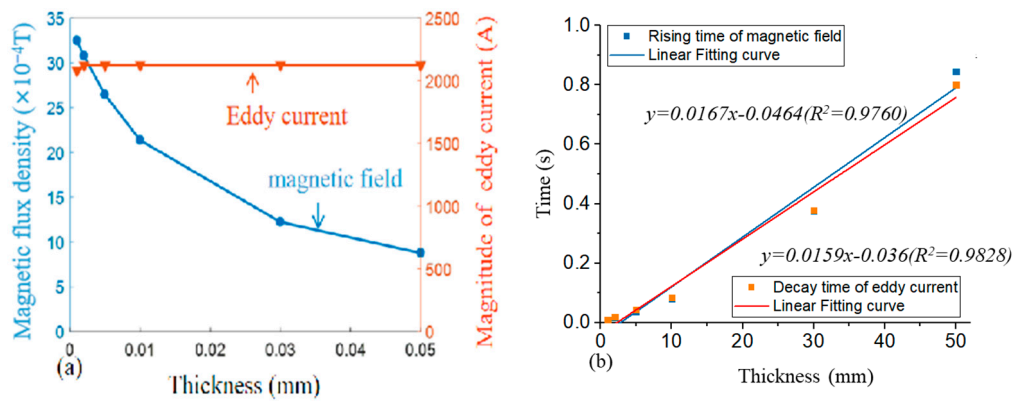


Figure 9. The magnitude (a) and characteristic time (b) of magnetic flux density and eddy current at different thicknesses.

3.4. Effects of Scaling Factors: The Scaling Criterion

Up to this point, all numerical analyses have been based on a structure with a length scale of approximately 1 m. However, the actual size of the ferromagnetic ship body will be 1–2 orders of magnitude larger than the numerical model. Understanding the impact of scaling factors is crucial for the design of the degaussing system. Consequently, further parametric analysis is conducted by varying the length scale of the structure. Two categories of scaled models are explored, depending on whether the shell thickness is scaled. Let us examine each type of scaled model separately.

3.4.1. The Scaled Model with Unchanged Thickness

In this case, the thickness of the structure remains the same. Table 4 presents four length-scale ratios that are used to analyze the scale effects parametrically. These ratios correspond to 1, 2, 5, and 10 times the base-line model. While the thickness is kept at 30 mm, the length and radius of the model are scaled accordingly. Figure 10 illustrates the dynamic responses of the magnetic flux density and the eddy current waveform under different scale ratios. Additionally, Figure 11 explicitly depicts the variations in amplitude and time constant of the magnetic field and the eddy current waveform with respect to the scale ratio.

Table 4. The dimensions and electromagnetic parameters of the model.

Scaling Ratio	Radius	Height	Thickness	Conductivity	Relative Permeability
1, 2, 5, 10	0.3 m × ratio	1.2 m × ratio	30 mm	5.9×10^6 S/m	80

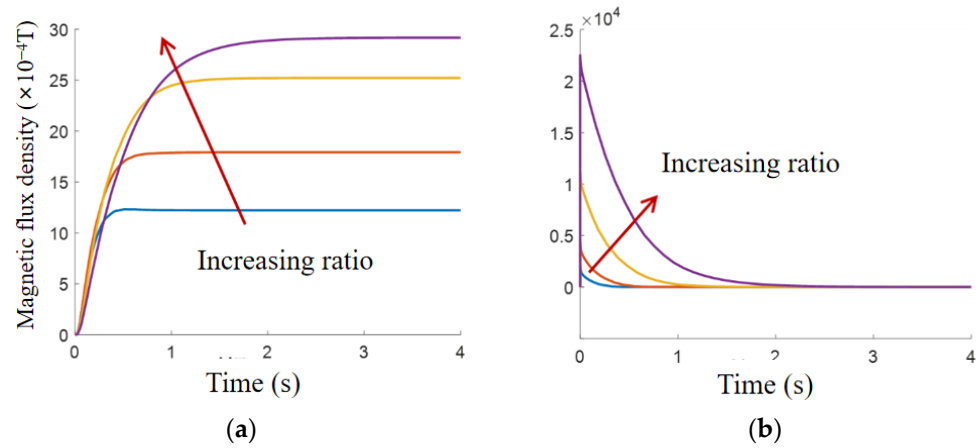


Figure 10. The changes in magnetic flux density (a) and eddy current (b) at different scaling ratio (unchanged thickness).

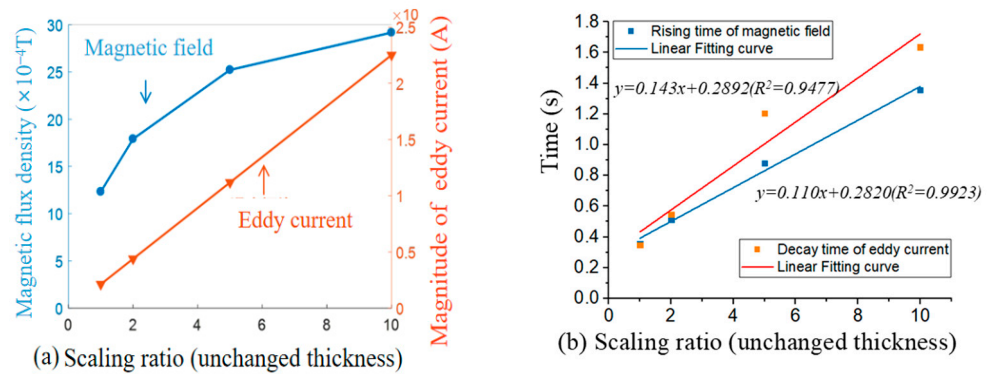


Figure 11. The magnitude (a) and characteristic time (b) of magnetic flux density and eddy current at different scaling ratio (unchanged thickness).

It can be noted that the scale ratio does significantly affect the rise time of the magnetic field and the decay time of the eddy current (as shown in Figure 11b). More importantly, the time constant for both the magnetic field and the eddy currents exhibits a clear linear relationship with the scale ratio, with reasonably good agreement. This observation confirms the deduction made in Equation (5) regarding the proportional relationship between the time constant and the scale ratio (b).

3.4.2. The Scaled Model with Equally Scaled Thickness

In this case, the thickness of the structure is simultaneously scaled. Table 5 presents four length-scale ratios used for parametric analysis, similar to the previous case. Figure 12 demonstrates the dynamic responses of the magnetic flux density and the eddy current waveform under different scale ratios, while Figure 13 explicitly illustrates the variations in amplitude and time constant of the magnetic field and the eddy current waveform with respect to the scale ratio.

Table 5. The dimensions and electromagnetic parameters of the model.

Scaling Ratio	Radius	Height	Thickness	Conductivity	Relative Permeability
1, 2, 5, 10	0.3 m × ratio	1.2 m × ratio	3 mm × ratio	5.9×10^6 S/m	80

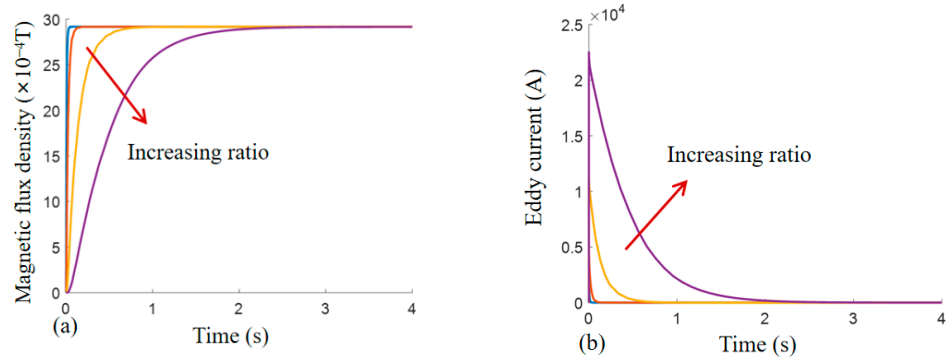


Figure 12. The changes in magnetic flux density (a) and eddy current (b) at different scaling scales (equally scaled thickness).

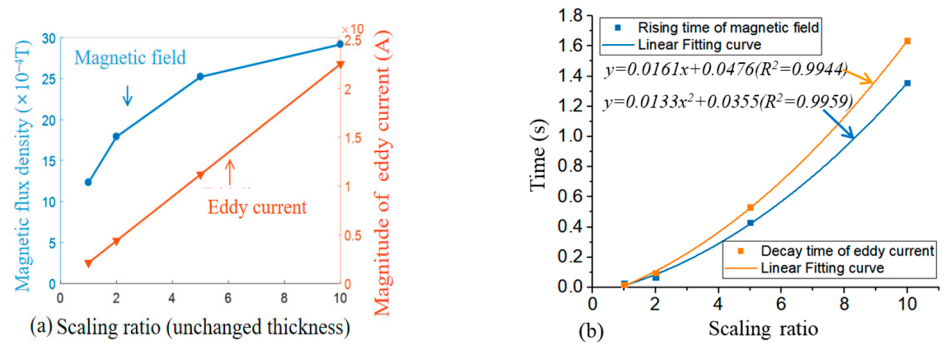


Figure 13. The magnitude (a) and characteristic time (b) of magnetic flux density and eddy current at different scaling scales (equally scaled thickness).

It is noteworthy that the scale ratio significantly affects the rise time of the magnetic field and the decay time of the eddy current (as shown in Figure 13b). Moreover, the time constant for both the magnetic field and the eddy currents exhibits a clear quadratic relationship with the scale ratio, showing good agreement. This observation further confirms the deduction made in Equation (5) regarding the proportional relationship between the time constant and the scale ratio (bc).

Based on the investigations of the single-layer structure mentioned above, the proposed eddy current mechanism model (Equation (5)) accurately depicts the correlation between the magnetic field response and the induced eddy current. Additionally, it effectively represents the effects of the geometry and physical parameters on the dynamics of the magnetic fields.

4. Validation on the Eddy Current Mechanism Model II: Multi-Layer Ferromagnetic Structure

4.1. Basic Examples

In addition to the single-layer ferromagnetic structure, a multi-layer ferromagnetic structure was also utilized to further validate its effectiveness. Figure 14 and Table 6 present the system parameters for the adopted multi-layer structure model. Compared to the single-layer ferromagnetic structure, the multi-layer configuration consists of three cylindrical layers with six bulkheads in the cylindrical chamber.

Table 6. The dimensions and electromagnetic parameters of the model.

Radius	Height	Thickness	Conductivity	Relative Permeability
0.3 m	1.2 m	30 mm	5.9×10^6 S/m	80

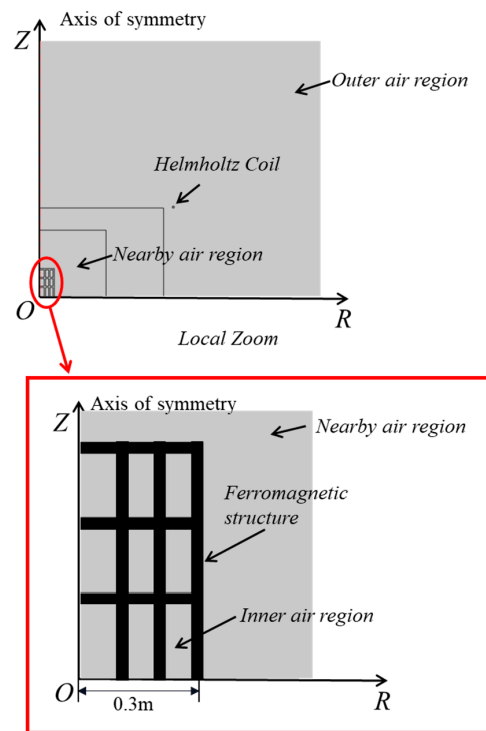


Figure 14. 2-dimensional axisymmetric model of multi-layer complex ferromagnetic structure.

4.2. Effects of Different Parameters on the Dynamic Magnetic Field Response

Using the developed COMSOL model, we conducted a quantitative evaluation of the effects of system parameters on the time constants for the magnetic field and the induced eddy current. The parameter setup follows that used in Section III. Figure 15 illustrates the variations of the time constant of the magnetic field and the eddy current with respect to the system parameters.

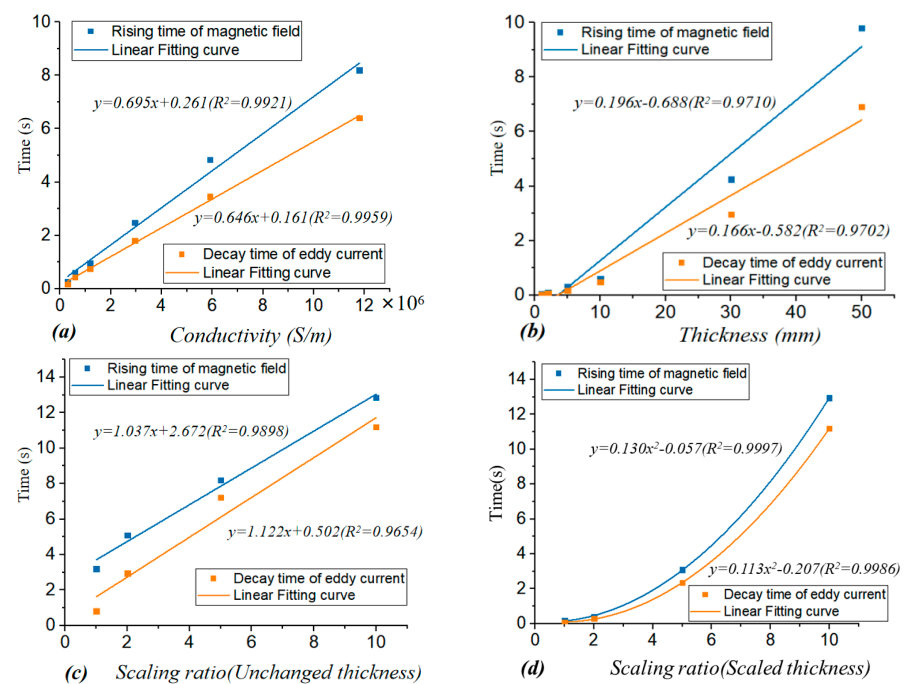


Figure 15. Effects of different system parameters on the characteristic time of the magnetic flux density and the eddy current: (a) Conductivity; (b) Thickness; (c) Scaling ratio (unchanged thickness); (d) Scaling ratio (scaled thickness).

It is noteworthy that the time constant of the multi-layer structure exhibits a similar variation pattern to that of the single-layer structure. In all cases, the magnetic field exhibits a time constant similar to that of the eddy current. The time constant shows a linear relationship with the structure's conductivity, thickness, and scale ratio (with thickness unchanged), and a quadratic relationship with the scale ratio (with thickness adjusted accordingly). These relationships are in line with the deductions made in the proposed eddy current mechanism model (Equation (5)), thereby validating the effectiveness of the proposed eddy current model for relatively complex structure models.

5. Conclusions

Towards providing theoretical guidance for modeling the dynamic magnetic field response in complex ship ferromagnetic metal structures, this paper introduces a general scaling criterion for dynamic magnetic field response in such structures, addressing the knowledge gap regarding the effects of eddy currents in the degaussing process. Based on this, the following key conclusions can be drawn:

- The proposed eddy current mechanism model, which employs a one-order LR circuit accounting for the influences of system physical and geometry parameters, demonstrates significant potential for practical engineering applications. It facilitates model simplification, enables the construction of physically scaled models, and allows for the quick assessment of dynamic magnetic field responses.
- The mechanism model deduces a linear relationship between the time constant of the dynamic magnetic field response and the conductivity, thickness, and length-scale (with unchanged thickness) while exhibiting a quadratic relationship with the scale ratio (with thickness adjusted accordingly).
- The effectiveness of the proposed mechanism model has been convincingly validated using ferromagnetic metal structures of varying complexity. Both single-layer and multi-layer ferromagnetic metal structures exhibit strong agreement with the proposed mechanism model, thereby confirming its effectiveness.
- In summary, the proposed eddy current mechanism model offers valuable insights and practical utility for understanding and predicting the dynamic magnetic field response in complicated ship ferromagnetic metal structures. Its successful validation through various structure configurations further enhances its reliability and applicability.

Author Contributions: Methodology, C.Z.; Validation, Z.L.; Investigation, Z.W. and W.Y.; Resources, H.X.; Data curation, J.W.; Writing—review & editing, M.C.; Supervision, P.G. All authors have read and agreed to the published version of the manuscript.

Funding: This research received no external funding.

Data Availability Statement: Data are contained within the article.

Conflicts of Interest: The authors declare no conflict of interest.

References

1. Hirota, M.; Furuse, T.; Eban, K.; Kubo, H.; Tsushima, K.; Inaba, T.; Shima, A.; Fujinuma, M.; Tojyo, N. Magnetic detection of a surface ship by an airborne LTS squid mad. *IEEE Trans. Appl. Supercond.* **2001**, *11*, 884–887. [[CrossRef](#)]
2. Nain, H.; Isa, M.; Muhammad, M.; Hassanudd, N.; Yusoff, N.; Yati, M.; Nor, I. Management of naval vessel's electromagnetic signatures: A review of sources and countermeasures. *Defence S&T Tech. Bull.* **2013**, *6*, 93–110.
3. Holmes, J.J. *Exploitation of a Ship's Magnetic Field Signatures*; Synthesis Lectures on Computational Electromagnetics; Springer: Cham, Switzerland, 2006; Volume 1, pp. 1–78.
4. Zhifei, W. Overview on the ship degaussing system. *Mar. Electr. Electron. Eng.* **2020**, *40*, 4–7.
5. Wikkerink, D.; Mor, A.R.; Polinder, H.; Ross, R. Magnetic signature reduction by converter switching frequency modulation in degaussing systems. *IEEE Access* **2022**, *10*, 74103–74110. [[CrossRef](#)]
6. Holmes, J.J. *Reduction of Ships Ferromagnetic Signatures*; Synthesis Lectures on Computational Electromagnetics; Springer: Cham, Switzerland, 2008; Volume 3, pp. 1–67.
7. Chung, H.J.; Yang, C.S.; Jung, W.J. A magnetic field separation technique for a scaled model ship through an Earth's magnetic field simulator. *J. Magn.* **2015**, *20*, 62–68. [[CrossRef](#)]

8. Modi, A.; Kazi, F. Magnetic-Signature Prediction for Efficient Degaussing of Naval Vessels. *IEEE Trans. Magn.* **2020**, *56*, 1–6. [[CrossRef](#)]
9. Swisulski, D.; Jakubiuk, K.; Zimny, P.; Woloszyn, M. Investigations of magnetic field of model of ship during degaussing process. *Prz. Elektrotechniczny* **2010**, *86*, 115–117.
10. Modi, A.; Kazi, F. Electromagnetic signature reduction of ferromagnetic vessels using machine learning approach. *IEEE Trans. Magn.* **2019**, *55*, 1–6. [[CrossRef](#)]
11. Choi, N.S.; Jeung, G.; Yang, C.S.; Chung, H.J.; Kim, D.H. Optimization of degaussing coil currents for magnetic silencing of a ship taking the ferromagnetic hull effect into account. *IEEE Trans. Appl. Supercond.* **2012**, *22*, 4904504. [[CrossRef](#)]
12. Kamal, M.; Daehn, G.S. A uniform pressure electromagnetic actuator for forming flat sheets. *J. Manuf. Sci. Eng.* **2007**, *129*, 369. [[CrossRef](#)]
13. Lai, Z.; Cao, Q.; Han, X.; Chen, M.; Liu, N.; Li, X.; Cao, Q.; Huang, Y.; Chen, Q.; Li, L. Insight into analytical modeling of electromagnetic forming. *Int. J. Adv. Manuf. Tech.* **2019**, *101*, 2585–2607. [[CrossRef](#)]
14. Kalantarov, C.T. *Handbook of Inductance Calculation*; China Machine Press: Beijing, China, 1992.
15. Guanghan, T.; Jianhua, K. A fast calculating method for magnetic field of solenoid. *Trans. China Electro Techn. Soc.* **1993**, *8*, 36–40.
16. Fawzi, T.H.; Buke, P.E. The accurate computation of self and mutual inductances of circular coils. *IEEE Trans. Power Apparatus Syst.* **1987**, *97*, 464–468. [[CrossRef](#)]
17. Zuo, C.; Wang, Z.; Yang, W.; Ruan, J.; Tang, L. Research on Inductance Calculations for Degaussing Windings of a Double-layer Steel Cylinder. *IEEE Access* **2021**, *9*, 55205–55213. [[CrossRef](#)]
18. Chen, D.X.; Brug, J.A.; Goldfarb, R.B. Demagnetizing factors for cylinders. *IEEE Trans. Magn.* **1991**, *27*, 3601–3619. [[CrossRef](#)]
19. Chen, D.X.; Pardo, E.; Sanchez, A. Fluxmetric and magnetometric demagnetizing factors for cylinders. *J. Magn. Magn. Mater.* **2006**, *306*, 135–146. [[CrossRef](#)]
20. Parq, J.H. Magnetometric demagnetization factors for hollow cylinders. *J. Magn.* **2017**, *22*, 550–556. [[CrossRef](#)]

Disclaimer/Publisher’s Note: The statements, opinions and data contained in all publications are solely those of the individual author(s) and contributor(s) and not of MDPI and/or the editor(s). MDPI and/or the editor(s) disclaim responsibility for any injury to people or property resulting from any ideas, methods, instructions or products referred to in the content.